The Cleavage Step of Ribonuclease P Catalysis Is Determined by Ribozyme−Substrate Interactions both Distal and Proximal to the Cleavage Site†

Andrew Loria and Tao Pan*

Department of Biochemistry & Molecular Biology, University of Chicago, Chicago, Illinois 60637

Received March 24, 1999; Revised Manuscript Received May 14, 1999

ABSTRACT: The cleavage step of bacterial RNase P catalysis involves concentration-independent processes after the formation of the ribozyme−substrate complex that result in the breaking of a phosphodiester bond. The 2′OH group at the cleavage site of a pre-tRNA substrate is an important determinant in the cleavage step. We determined here that in contrast to a tRNA substrate, the 2′OH at the cleavage site of two in vitro selected substrates has no effect, whereas a 2′OH located adjacent to the cleavage site has a similarly large effect on the cleavage step. This result indicates that a unique 2′OH in the vicinity of the cleavage site interacts with the ribozyme to achieve the maximal efficiency of the cleavage step. Individual modifications in a pre-tRNA substrate that disrupt ES interactions proximal to the cleavage site generally have little effect on the usage of this unique 2′OH. Ribozyme modifications that delete the interactions involving the T stem−loop of the tRNA have a large effect on the usage of this unique 2′OH and also alter the location of this 2′OH. We propose a new ES complex prior to the bond-breaking step in the reaction scheme to explain these results. This second ES complex is in fast equilibrium with the initial ES complex formed by bimolecular collision. The ribozyme interaction with this unique 2′OH shifts the equilibrium in favor of the second ES complex. The formation of the second ES complex may require optimal geometry of the two independently folding domains of this ribozyme to precisely position crucial functional groups and Mg^{2+} ions in the active site. Such a domain geometry is significantly favored by the RNase P protein. In the absence of the protein, spatial rearrangement of these domains in the ES complex may be necessary.

The catalysis of biological ribozymes can often be described by two or more distinct events after the formation of the bimolecular ribozyme−substrate complex. Starting with the ES complex described by the crystal structures (*1, 2*), the hammerhead ribozyme is thought to undergo a conformational change prior to breaking the phosphodiester bond (*3, 4*). This conformational change may involve structural rearrangements to position crucial functional groups and/or Mg^{2+} ions in the active site. Starting with the ES complex formed initially through Watson−Crick base pairs, the group I ribozyme docks the helix containing the substrate into the catalytic core involving a large-scale movement of this helix prior to the transesterification reaction (*4*−*7*). The bond-breaking step in both ribozymes presumably follows the conformational change and is catalyzed by Mg^{2+} ions.

The cleavage reaction by the ribozyme from bacterial RNase P may also involve two distinct events after the bimolecular collision to form the ES complex. RNase P is an essential endoribonuclease responsible for producing the mature 5′ end of all tRNAs in vivo (*8, 9*). The bacterial RNase P is composed of one small protein (∼13−15 kDa) and one large RNA (∼330−420 nucleotides) which is capable of catalysis in the absence of the protein (*10*). We have shown previously that the substitution of the 2′OH group at the cleavage site of a pre-tRNA^{Phe} substrate to 2′H decreased the cleavage rate by ∼240-fold in the RNA alone (denoted P RNA)[1] and ∼30-fold in the RNA/protein (denoted holoenzyme) reaction (*11, 12*). This 2′OH to 2′H substitution decreased the cleavage rate at two miscleavage sites by the same magnitude, whereas substitution of 2′OH to 2′H at both miscleavage sites had no effect on cleavage at any site (*11, 12*). A simple interpretation of this result suggests two conformationally distinct ES complexes (designated as ES_1 and ES_2), and the ribozyme interaction with this 2′OH facilitates the ES_1-to-ES_2 transition. This structural transition presumably precedes the bond-breaking event of the RNase P reaction, proposed to be catalyzed by at least two Mg^{2+} ions (*13, 14*).

This paper describes ribozyme−substrate interactions that determine the choice of a catalytically important 2′OH group in the substrate (designated as 2′OH*) and a possible structural transition between two ES complexes prior to the bond-breaking event. A model for the structural differences among these two ES complexes is proposed. We first

† This work was supported by a grant from the NIH (GM52993).

* Corresponding author. Telephone: (773)702-4179. Fax: (773)-702-0439. E-mail: taopan@midway.uchicago.edu.

[1] Abbreviations: C-domain or catalytic domain, originated from a circularly permuted P RNA with the 5′ end at nucleotide 240 (the C-domain contains nucleotides 240−409 + 1−85 of *B. subtilis* P RNA); c^0, cleavage site between nucleotides −1 and +1 of the pre-tRNA^{Phe} substrate; holoenzyme, 1:1 complex between RNA and the protein component of *B. subtilis* RNase P; P RNA, RNA component of *B. subtilis* RNase P; m^2, cleavage site between nucleotides +2 and +3 of the pre-tRNA^{Phe} substrate; S-domain or specificity domain, nucleotides 86−239 of *B. subtilis* P RNA; 2′OH*, single 2′OH group in the substrate that confers a large effect on the cleavage rate.

10.1021/bi990691f CCC: $18.00
Published on Web 06/12/1999

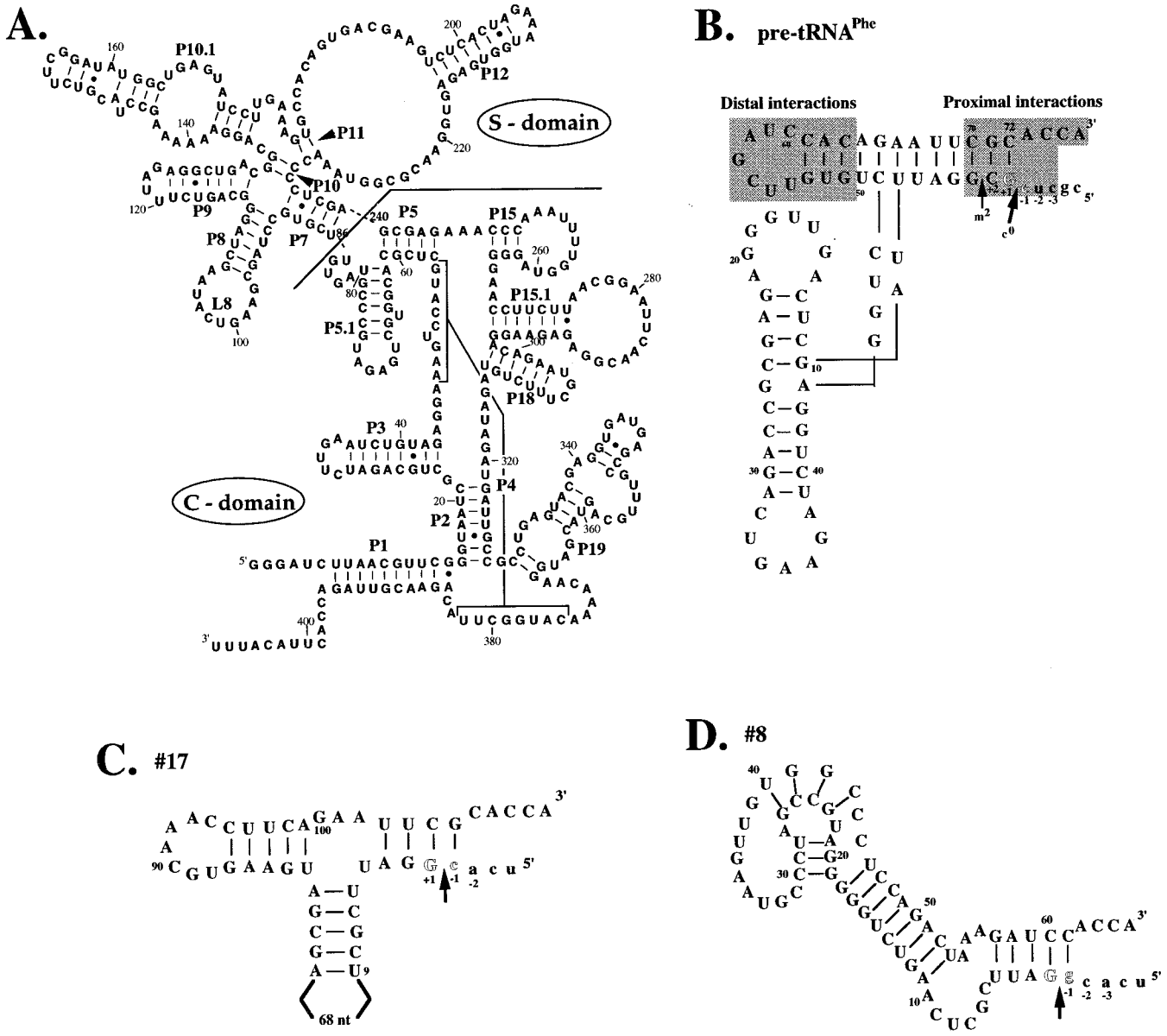

FIGURE 1: (A) Independently folding domains of *B. subtilis* P RNA. The catalytic domain (C-domain) contains nucleotides 240−409 + 1−85. The specificity domain (S-domain) contains nucleotides 86−239. (B) L-representation of the pre-tRNA^{Phe} substrate. The RNase P ribozyme only interacts with the T stem−loop and the acceptor stem of the tRNA. The correct cleavage site (c^0 site) is indicated by a thick arrow, and the miscleavage site (m^2 site) is indicated by a thin arrow. Nucleotides in the 5′ leader are shown in lower case letters. The distal interactions involve nucleotides in the T stem−loop region, whereas the proximal interactions involve nucleotides in the 5′ leader, the 3′CCA, and the 1·72 base pair. (C and D) Secondary structures of the two selected substrates used in this work. Only the portion in substrate #17 that directly interacts with P RNA is shown (*22*).

demonstrate with two in vitro selected substrates that the 2′OH* does not need to coincide with, but is adjacent to the cleavage site. The selection of a particular 2′OH to be used as 2′OH* in a pre-tRNA^{Phe} substrate is determined by ribozyme−substrate interactions that are both distal and proximal to the cleavage site. Similar results obtained in the presence of the RNase P protein suggest a role of this protein in the facilitation of the ES_1-to-ES_2 transition.

MATERIALS AND METHODS

Preparation of RNA Substrates. All pre-tRNA substrates were made by ligating a synthetic oligoribonucleotide containing either zero, one, or two 2′-deoxynucleotides to an RNA transcript containing nucleotides 10−76 of yeast tRNA^{Phe} (Figure 1B) as described previously (*11*, *15*). The selected substrates were prepared by ligating a synthetic oligoribonucleotide containing either zero or one 2′-deoxynucleotide to an RNA transcript containing nucleotides 7−113 of substrate #17 and nucleotides 6−65 of substrate #8 [Figure 1C,D (*16*, *17*)]. All RNA oligonucleotides were custom-synthesized by Dharmacon Research (Boulder, CO) using novel 2′ protecting groups. The DNA oligonucleotide splint used for ligating the #17 substrate, 5′CGTACTTGAGCGAATCCGTGA, is complementary to nucleotides −5 to +17, and that for ligating the #8 substrate, 5′GATCGGCATCCCCCAGACTTGAGCGAATCCGTGA, is complementary to nucleotides −5 to +29.

C-Domain of P RNA. The C-domain construct used in this work originated from a circularly permuted form of P RNA with the 5′ end at nucleotide 240 (Figure 1A). Nucleotides

86−239 of the *B. subtilis* P RNA are deleted from this circularly permuted P RNA to generate a C-domain construct with the 5′ end at nucleotide 240 and the 3′ end at nucleotide 85. This construct is independently folded at comparable Mg^{2+} concentrations ($K_{Mg}^{folding} \sim 1.3$ mM) as the full-length P RNA ($K_{Mg}^{folding} \sim 0.8$ mM) (*18, 19*). The C-domain was transcribed from a T7 RNA polymerase promoter, purified by denaturing gel electrophoresis, and stored in water. The RNA was renatured by heating in the reaction buffer (generally 50 mM trisHCl, pH 8.1, or 50 mM MES, pH 6.1) for 2 min at 90 °C, followed by 3 min incubation at room temperature. Mg^{2+} was then added to appropriate concentrations and the mixture incubated at 37 or 50 °C for 5 min.

Ribozyme Preparation with P Protein. The *B. subtilis* P protein was overexpressed and purified from *E. coli* as described by the Fierke lab (*20*). The holoenzyme was reconstituted as described (*12*) and was always at 1 mol of P protein/1 mol of P RNA. For the C-domain reactions, the P protein was added to the previously renatured C-domain at 10 mM $MgCl_2$ at the ratio of one protein per RNA and the mixture incubated at 37 °C for an additional 5 min.

Kinetics of the Cleavage Reaction. All kinetic reactions were performed under single turnover conditions with 500−20 000-fold molar excess of ribozyme over 5′-^{32}P-labeled substrates. The final concentrations of the ribozyme range from 0.5 to 20 μM. All reactions with pre-tRNA substrates were carried out at 37 °C in 50 mM MES, pH 6.1, or trisHCl, pH 8.1, 100 mM $MgCl_2$, 0.6 M KCl for reactions without the P protein and 50 mM MES, pH 6.1, or TrisHCl, pH 8.1, 10 mM $MgCl_2$, 2% glycerol for reactions with the P protein. The reaction conditions for the selected substrates are listed in Table 1.

The details of kinetic reactions and data processing were identical to those described earlier (*11, 12*). Similar to the early studies, the cleavage sites at the correct (between nucleotides −1 and +1, Figure 1B) and incorrect (between nucleotides +2 and +3) positions are designated as c^0 and m^2 sites, respectively. The reaction rates were determined using equations for parallel reactions (*21*). First, the amounts of individual reaction products [$cpm(P)_t$] and remaining substrate [$cpm(S)_t$] were quantitated. The sum of the cleavage rates (k_{cl}) was obtained by fitting [fraction S remaining](t) = $cpm(S)_t/[cpm(S)_t + \Sigma cpm(P)_t]$ versus time (t) with a single-exponential function. The reaction rates for individual cleavage sites were calculated according to

$$k_{cl} = k_{cl}^{c0} + k_{cl}^{m2} \quad (1)$$

$$k_{cl}^{c0} = [cpm(P)_t^{c0}/\Sigma cpm(P)_t]k_{cl} \quad (2)$$

$$k_{cl}^{m2} = [cpm(P)_t^{m2}/\Sigma cpm(P)_t]\, k_{cl} \quad (3)$$

At least two ribozyme concentrations that differed by 5−10-fold were used in every reaction to ensure that the observed rate at the higher enzyme concentration was close to saturation. Although saturation was obtainable in all but one case described here, it was necessary to use different ionic conditions for reactions with or without the P protein. This limitation, however, should not significantly affect our conclusions which are based on comparing the cleavage rates among substrates containing a single 2′H substitution. In the C-domain reaction without the P protein, the observed cleavage rate at the highest ribozyme concentration used (20 μM) was ∼2-fold less than the calculated cleavage rate at the saturating C-domain concentration.

Table 1: Effect of 2′OH → 2′H Substitutions on the Chemical Step of Two in Vitro Selected Substrates

substrate	k_{cl} (min^{-1}) (P RNA)[a]	$\Delta\Delta G^c$ (kcal/mol)	k_{cl} (min^{-1}) (holoenzyme)[b]	$\Delta\Delta G^c$ (kcal/mol)
#17 (all-ribo)	5.3 ± 0.4	−	8.7 ± 1.2	−
2′H (+1)	2.0 ± 0.2	0.6	2.6 ± 0.2	0.7
2′H (−1)	2.6 ± 0.2	0.4	4.4 ± 0.2	0.4
2′H (−2)	0.047 ± 0.003	**2.9**	0.67 ± 0.02	**1.6**
#8 (all-ribo)	0.90 ± 0.13	−	2.6 ± 0.4	−
2′H (−1)	0.65 ± 0.11	0.2	1.4 ± 0.1	0.4
2′H (−2)	<0.0002	>**5.0**	0.063 ± 0.006	**2.3**
2′H (−3)	0.31 ± 0.01	0.7	4.0 ± 1.6	−0.3

[a] k_{cl} represents the cleavage rate at saturating ribozyme concentrations (5 μM E and ∼1 nM S). Conditions: substrate #17 at 50 mM MES, pH 6.7, 50 mM $MgCl_2$, 37 °C; substrate #8 at 50 mM MES, pH 6.7, 10 mM $MgCl_2$, 1 mM spermine, 37 °C. [b] Conditions: substrate #17 at 50 mM MES, pH 6.7, 10 mM $MgCl_2$, 37 °C; substrate #8 at 50 mM MES, pH 6.7, 10 mM $MgCl_2$, 1 mM spermine, 37 °C. [c] $\Delta\Delta G = -RT \ln [k_{cl}(2'H)/k_{cl}(\text{all-ribo})]$. The boldfaced $\Delta\Delta G$ values indicate the utilization of the 2′OH at the −2 positions as the 2′OH*.

RESULTS

Effect of Single 2′OH → 2′H Substitutions around the Cleavage Site of Selected Substrates. The model for cleavage site selection proposed in our previous work (*11*) suggests that the choice of 2′OH* does not have to depend on the location of the cleavage site. In the case of the pre-tRNA^{Phe} substrate, the 2′OH* coincides with the correct cleavage site, but not with the miscleavage sites. Two in vitro selected substrates are used to test whether the 2′OH* phenomenon is general for other RNase P substrates. These two substrates are among the best characterized substrates from in vitro selection, and they show no detectable miscleavage (*17, 22*). Unlike the pre-tRNA substrate where the correct cleavage site is at the end of the acceptor stem, the single cleavage sites in these selected substrates are located between the first and the second base pair of a short helix (Figure 1C,D). Single 2′OH → 2′H substitutions in both substrates show that the 2′OH group at the cleavage site (−1 position) has no effect on the cleavage rate in both P RNA and holoenzyme reactions ($\Delta\Delta G$ = 0.2−0.4 kcal/mol, Table 1). In contrast, the 2′OH → 2′H substitution at the −2 position in both substrates decreases the cleavage rates significantly ($\Delta\Delta G$ = 2.9−5.0 kcal/mol for P RNA and $\Delta\Delta G$ = 1.6−2.3 kcal/mol for holoenzyme reactions, boldfaced $\Delta\Delta G$ values in Table 1). The extent of these large decreases is comparable to the 2′OH* → 2′H substitution in the pre-tRNA substrate [$\Delta\Delta G$ = 3.4 kcal/mol for P RNA and $\Delta\Delta G$ = 2.1 kcal/mol for holoenzyme reactions (*11, 12*)]. As a control, one other substitution at either the −3 or the +1 position has only a small effect on the cleavage rate (Table 1). These results indicate that a unique 2′OH is utilized as 2′OH* in the selected substrates and the 2′OH* does not coincide with the cleavage site.

Effects of Substrate Modifications Proximal to the Cleavage Site. Our previous model for the cleavage step of a pre-tRNA substrate suggests that even though the choice of the 2′OH* is not determined by the location of the cleavage site, the 2′OH* is still confined in the vicinity of the cleavage

Table 2: Effect of 5′ Leader/3′ CCA Deletions and 1·72 Mismatches on the Chemical Step of a Pre-tRNA^{Phe} Substrate

substrate	k_{cl} (min^{-1}) (P RNA)[a]	ΔΔG (kcal/mol)	k_{cl} (min^{-1}) (holoenzyme)[b]	ΔΔG (kcal/mol)
5′-cgcuc-tRNA	1.8 ± 0.1	–	2.6 ± 0.3	–
2′H (−1)	0.0076 ± 0.0002	3.4	0.081 ± 0.006	2.1
ΔCCA	1.0 ± 0.1	0.4 [3.8][c]	1.7 ± 0.1	0.3 [2.7][c]
Δ−5, −4	3.5 ± 0.2	−0.4 [3.8]	3.5 ± 0.2	−0.2 [2.0]
Δ−5, −4, −3, −2	1.0 ± 0.1	0.4 [5.0]	0.5 ± 0.2	1.0 [>6.0]
G1·A72 (all-ribo)	1.3 ± 0.1	0.2 (−)[c]	1.2 ± 0.1	0.5 (−)[c]
G1·A72 (2′H(−1))	0.0033 ± 0.0002	(3.7)	0.013 ± 0.002	(2.8)
G1·U72 (all-ribo)	0.93 ± 0.03	0.4 (−)	1.4 ± 0.1	0.4 (−)
G1·U72 (2′H(−1))	0.0010 ± 0.0002	(4.2)	0.0024 ± 0.0008	(3.9)

[a] Conditions: 50 mM MES, pH 6.1, 100 mM $MgCl_2$, 0.6 M KCl, 37 °C. [b] Conditions: 50 mM MES, pH 6.1, 10 mM $MgCl_2$, 37 °C. [c] In brackets: $-RT \ln [k_{cl}(\Delta,2'H)/k_{cl}(w.t.,2'OH)]$; data for the 2′H substrates are taken from (*11, 12*). In parentheses: $-RT \ln [k_{cl}(2'H)/k_{cl}(2'OH)]$. The $\Delta\Delta G$ values of >3.0 kcal/mol for the P RNA and >2.0 kcal/mol for the holoenzyme reactions indicate that the 2′OH at the cleavage site of these modified pre-tRNA substrates is still used as 2′OH*.

site (*11*). Hence, the cleavage site is used here as a reference point for our modifications. Two types of ribozyme−substrate interactions can be proposed for the selection of the 2′OH*. The first type involves the ribozyme interaction with functional groups in the substrate proximal to the cleavage site. The proximal interactions include the 3′CCA, the 5′ leader (−5 to −1 nucleotides), and the 1·72 base pair in the pre-tRNA substrate [Figure 1B (*8, 11, 23*−*26*)]. The second type involves the ribozyme−substrate interactions distal to the cleavage site. The distal interactions include the T stem−loop in the pre-tRNA substrate [Figure 1B (*15, 27*−*29*)].

To test for contributions from proximal interactions in selecting the 2′OH*, cleavage rates for substrates containing deletions or mutations are determined and compared to that of the unmodified pre-tRNA^{Phe} substrate (Table 2). The 2′OH* → 2′H substitution decreased the cleavage rate by ∼240-fold (3.4 kcal/mol) for the P RNA or ∼30-fold (2.1 kcal/mol) for the holoenzyme reaction (*11, 12*). If an important contributor in the substrate is deleted or altered to result in the loss of the 2′OH* interaction, the cleavage rate should be decreased by a similar magnitude as the 2′OH* → 2′H substitution (i.e., 3.4 or 2.1 kcal/mol).

The contribution of 3′CCA and the 5′ leader in selecting the 2′OH* is determined using substrates containing 3′ or 5′ deletions. When 3′CCA or the −5 to −2 nucleotides in the 5′ leader are deleted, the effects on the cleavage rates are much smaller than 3.4 kcal/mol for the P RNA and 2.1 kcal/mol for the holoenzyme reactions (Table 2). When the 2′OH at the −1 position is changed to 2′H in the substrates containing 3′CCA or 5′ leader deletions, the cleavage rates are decreased by >420-fold (3.8 kcal/mol) for P RNA and >26-fold (2.0 kcal/mol) for holoenzyme reactions (Table 2, $\Delta\Delta G$ in brackets). These results indicate that the pre-tRNA substrates with 3′CCA and 5′ leader deletions still employ the same 2′OH* as the wild-type substrate.

Although the Watson−Crick base pairs for the 1·72 nucleotides are universal, their sequences are not conserved among natural tRNAs (∼70% G1·C72 and 30% others (*30*)]. Since 2′OH groups are conserved in natural pre-tRNA substrates, the choice for 2′OH* is unlikely to be determined by an entity not present in all tRNAs. Therefore, the possibility for the sequence identity of the 1·72 Watson−Crick base pair to position 2′OH* was not tested experimentally.

Although the sequence of the 1·72 Watson−Crick base pair should not matter, the helical context of the 1·72 base pair may contribute to the selection of 2′OH*. The 2′OH* in a pre-tRNA substrate is uniquely located at the end of the acceptor stem helix. The effects of G1·C72 to G1·A72 and G1·U72 mutations show that the helical context is not a determining factor in selecting the 2′OH* (Table 2). With the all-ribo substrate, the effect of the 1·72 mismatch is less than 2-fold (0.5 kcal/mol) in all cases. When the 2′OH at the −1 position in 1·72 mismatched substrates is changed to 2′H, the cleavage rates are decreased by >390-fold (3.7 kcal/mol) for P RNA and >90-fold (2.8 kcal/mol) for holoenzyme reactions (Table 2, $\Delta\Delta G$ in parentheses). These results again indicate that the 2′OH* in the mismatched substrates is at the identical position as the wild-type substrate.

Effect of the 1·72 Mismatch on the Miscleavage at +2. As previously reported (*11, 12*), our pre-tRNA^{Phe} substrate miscleaves at nucleotides +2 and −2 at ∼1−10% of the cleavage at the correct site (nucleotide −1). The miscleavage reactions are extremely useful in understanding the 2′OH* utilization for cleavage at different sites (*11, 12*). Cleavage at the +2 nucleotide (designated as the m^2 site as in our previous work) can be accurately quantitated to illustrate how this ribozyme selects 2′OH* for the correct (designated as c^0) and m^2 sites. Since the selected substrates are not miscleaved, the c^0/m^2 nomenclature identifies the cleavage reaction of the pre-tRNA^{Phe} substrate in this work. We focus on the differential effects of 1·72 mismatches and 2′OH → 2′H substitutions on c^0 and m^2 cleavages (Table 3). Both C72 → A72 and C72 → U72 mutants show similar effects (not shown), and only the $\Delta\Delta G$ values for the G1·A72 substrate are given in Table 3 for clarity.

The G1·C72 → G1·A72, the 2′OH (c^0) → 2′H, and the 2′OH (m^2) → 2′H modifications can be considered as three components in determining the efficiency of the cleavage step. For c^0 cleavage, the only significant effect is the 2′OH (c^0) → 2′H modification (rows 1−3, Table 3). In all but one case, the effect of double modifications is additive in $\Delta\Delta G$, suggesting that these components act independently (rows 4−6, Table 3). For the holoenzyme reaction, simultaneous G1·C72 → G1·A72 and 2′OH (c^0) → 2′H modification has a slightly larger effect (3.3 kcal/mol) than the sum of the $\Delta\Delta G$ values of either modification alone (0.5 + 2.1 kcal/mol). This nonadditivity in $\Delta\Delta G$ suggests a small cooperativity in the ribozyme−substrate interactions involving the G1·C72 base pair and the 2′OH (c^0).

In contrast, both G1·C72 → G1·A72 and 2′OH (c^0) → 2′H modifications have large effects on m^2 cleavage. Simulta-

Table 3: Differential Effect of G1·C72 → G1·A72 Mutation and 2′OH → 2′H Substitutions of the Pre-tRNA^{Phe} Substrate on the c^0 and m^2 Cleavages

substrate modification	ΔΔ*G* (P RNA)[a]		ΔΔ*G* (holoenzyme)[a]	
	c^0	m^2	c^0	m^2
C72 → A72	0.2	1.8	0.5	2.1
2′OH (c^0) → 2′H[b]	3.4	3.3	2.1	2.3
2′OH (m^2) → 2′H[b]	−0.2	−0.1	−0.1	0.2
C72 → A72 and 2′OH (c^0) → 2′H	3.9	4.0	3.3	**2.4**
C72 → A72 and 2′OH (m^2) → 2′H	0.1	1.6	0.1	1.8
2′OH (c^0) → 2′H and 2′OH (m^2) → 2′H[b]	3.0	3.4	2.0	2.4
C72 → A72 and 2′OH(c^0) → 2′H and 2′OH(m^2) → 2′H	4.1	4.3	3.4	**5.5**

[a] $\Delta\Delta G = -RT \ln [k_{cl}(\text{modified})/k_{cl}(\text{w.t., all-ribo})]$, in kcal/mol. ΔΔ*G* > 0: the cleavage rate is decreased for the modified substrates. ΔΔ*G* < 0: the cleavage rate is increased for the modified substrates. Reaction conditions for P RNA: 50 mM MES, pH 6.1, 100 mM $MgCl_2$, 0.6 M KCl, 37 °C. Reaction conditions for holoenzyme: 50 mM MES, pH 6.1, 10 mM $MgCl_2$, 37 °C. [b] Data from (*11*, *12*). [c] The boldfaced ΔΔ*G* values for the holoenzyme reactions indicate utilization of 2′OH(m^2) as 2′OH* for m^2 cleavage when 1·72 is mismatched and the 2′ position is H at the c^0 position. See text for detailed explanation.

neous G1·C72 → G1·A72 and 2′OH (c^0) → 2′H modification has a significantly smaller effect (4.0 and 2.4 kcal/mol) than the additive ΔΔG of either modification alone (1.8 + 3.3 and 2.1 + 2.3 kcal/mol; Table 3). These results suggest that the large effect of either G1·C72 → G1·A72 or 2′OH (c^0) → 2′H modification alone on m^2 cleavage can be attributed to a partial loss of function of the unmodified entity [i.e., 2′OH (c^0) or G1·C72] upon modification of the other [i.e., G1·A72 or 2′H (c^0)]. There is, however, an alternative scenario in which the 2′OH at the m^2 site may be used as the 2′OH* for m^2 cleavage, only when the 1·72 nucleotides are mismatched *and* the c^0 site contains a 2′H. The holoenzyme reaction is consistent with this alternative interpretation: the triple modification, G1·C72 → G1·A72 and 2′OH (c^0) → 2′H and 2′OH (m^2) → 2′H, decreases the cleavage at the m^2 site by a much greater extent than the double modification, G1·C72 → G1·A72 and 2′OH (c^0) → 2′H (5.5 versus 2.4 kcal/mol). The triple and double modifications have essentially the same effect on the P RNA reaction (4.3 versus 4.0 kcal/mol), suggesting that the 2′OH (m^2) utilization as 2′OH* is unique for the holoenzyme reaction.

Effects of Ribozyme Modifications Distal to the Cleavage Site. Two types of experiments can be designed to test how ribozyme−substrate interactions distal to the cleavage site (Figure 1B) determine the choice of 2′OH*. The first type involves insertion or deletion of one base pair between the T stem−loop and the site of 2′OH* to shift the position of the 2′OH* by one nucleotide. Unfortunately, changing the number of base pairs in the T stem also alters the orientation of the T stem−loop to the D stem−loop and the variable loop in tRNA to result in misfolding (*31*, *32*). Hence, results from T stem insertion/deletion are unlikely to be conclusive due to the potential misfolding of tRNA (*33*). Insertion/deletion of one base pair in the acceptor stem essentially shifts the 5′ leader by one nucleotide and is almost equivalent to some natural pre-tRNA substrates where the −1 and +73 nucleotides are base paired. In all but one natural substrates, the −1·73 pair has little effect on cleavage efficiency (*34*, *35*). A pre-tRNA^{Phe} substrate in our previous work had a U1·A73 base pair, and this substrate has the identical 2′OH* as the C1·A73 substrate (*11*, *12*). Hence, changing the number of base pairs in the acceptor stem cannot provide direct evidence on the role of distal interactions.

A second type of experiment involves deletion of the distal interactions. At least three 2′OH groups in the T stem−loop have been identified to directly interact with the ribozyme, each contributing 1−2 kcal/mol in substrate binding (*12*, *15*). Single 2′H substitution of these 2′OH groups has, however, little effect on the cleavage rate. Therefore, elimination of multiple interactions in this region may be necessary to observe their collective effect on 2′OH* selection. Deletion of the distal interactions can be accomplished either by replacing the T stem−loop in the pre-tRNA substrate by a tetraloop or by deleting the specificity domain in the *B. subtilis* P RNA (nucleotides 86−239) which interacts with the T stem−loop (*27*−*29*). Since the tetraloop addition in a modified substrate may interfere with ribozyme activity, we choose to delete the S-domain originating from a circularly permuted P RNA (*36*, *37*). This construct (denoted as catalytic domain or C-domain) contains nucleotides 240−409 + 1−85 of the *B. subtilis* P RNA and folds stably and independently as analyzed by a variety of biochemical assays including hydroxyl radical protection and catalytic activity with the selected substrate #8 (*19*).

The C-domain accurately cleaves the pre-tRNA^{Phe} substrate in the absence and presence of the *B. subtilis* P protein (Figure 2 and Table 4). Furthermore, the C-domain reaction produces the same miscleavage pattern as the wild-type ribozyme. Cleavage by the C-domain in the presence of P protein requires less than 1 μM ribozyme to reach 50% of the maximal cleavage rate (Figure 2). In the absence of the P protein, ∼20 μM ribozyme is needed to reach 50% of the maximal cleavage rate (data not shown); 20 μM is the highest ribozyme concentration used in our experiments. Therefore, the cleavage rates can be accurately determined with the P protein and within 2-fold without the P protein (Table 4). Compared to the wild-type ribozyme, the cleavage rates are reduced by ∼25 000-fold for the C-domain reaction without the P protein and by only ∼40-fold with the P protein. The 2′OH (c^0) → 2′H substitution decreases the c^0 cleavage by ∼230-fold (3.3 kcal/mol) for the C-domain alone and ∼2200-fold (4.7 kcal/mol) for the reaction with P protein. On the other hand, the cleavage rate upon 2′OH (c^0) → 2′H substitution only decreases m^2 cleavage by ∼4−6-fold (0.8−1.1 kcal/mol) with or without the P protein (Table 4). When the 2′OH at the m^2 site is substituted with 2′H, m^2 cleavage decreases by ∼5-fold (0.9 kcal/mol) without and ∼42-fold (2.3 kcal/mol) with P protein, while the c^0 cleavage remains unaffected. These results show that deletion of the distal interactions changes the rule for the 2′OH* selection. For c^0

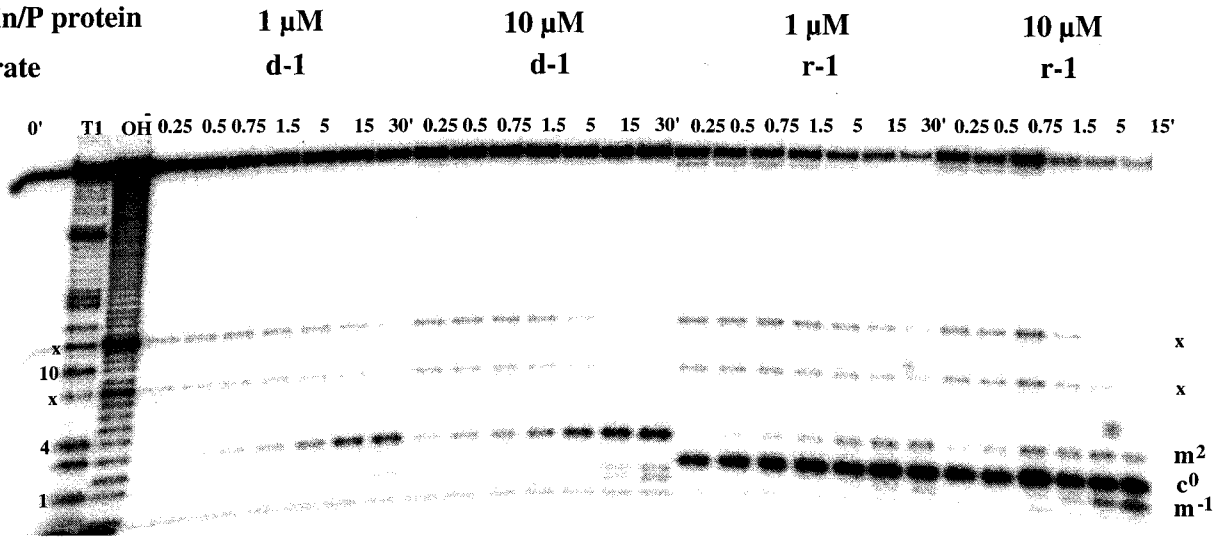

FIGURE 2: Cleavage of the pre-tRNA^{Phe} substrate by the *B. subtilis* C-domain in the presence of equal molar quantities of *B. subtilis* P protein. The substrate is 5′-^{32}P-labeled and has either a 2′H (d-1) or a 2′OH (r-1) at the c^0 site. The cleavage rates differ by less than 1.6-fold at 1 and 10 μM ribozyme concentrations. Therefore, the reactions at 10 μM ribozyme are considered to be at saturation. The reaction times are given in minutes above the labeled substrates. The three cleavage products are indicated at the right side. The bands labeled by "x" represent substrates that are nicked at U8A9 and U13A14 of tRNA^{Phe} prior to the addition of the ribozyme. These nicked substrates are only present in this particular substrate preparation and have no effect on the cleavage pattern. T1 and OH^-: partial nuclease T1 digestion and alkaline hydrolysis of the same substrate, respectively.

Table 4: Effect of S-Domain Deletion on the Chemical Step of a Pre-tRNA^{Phe} Substrate

substrate	cleavage site	k_{obs} (min^{-1}) (C-domain only)[a]	$\Delta\Delta G$ (kcal/mol)[c]	k_{cl} (min^{-1}) (+P protein)[b]	$\Delta\Delta G$ (kcal/mol)[c]
all-ribo	c^0	$(7.1 \pm 0.4) \times 10^{-3}$	−	13 ± 1	−
	m^2	$(0.22 \pm 0.08) \times 10^{-3}$	−	0.64 ± 0.26	−
2′OH(c^0)	c^0	$(0.031 \pm 0.017) \times 10^{-3}$	3.3	0.0058 ± 0.0017	4.7
→ 2′H	m^2	$(0.058 \pm 0.018) \times 10^{-3}$	0.8	0.10 ± 0.01	1.1
2′OH(m^2)	c^0	$(4.4 \pm 0.4) \times 10^{-3}$	0.3	13 ± 1	0.0
→ 2′H	m^2	$(0.048 \pm 0.021) \times 10^{-3}$	0.9	<0.06	>1.4
2′OH(c^0,m^2)	c^0	ND[c]		0.0057 ± 0.0012	4.7
→ 2′H	m^2			0.0024 ± 0.0010	3.4

[a] Conditions: 20 μM C-domain, 50 mM TrisHCl, pH 8.1, 100 mM $MgCl_2$, 0.6 M KCl, 37 °C. The k_{obs} is estimated to be within 2-fold of k_{cl}. [b] Conditions: 10 μM C-domain + P protein, 50 mM TrisHCl, pH 8.1, 10 mM $MgCl_2$, 37 °C. [c] The $\Delta\Delta G$ values for the 2′OH → 2′H substitution at the cleavage sites are underlined.

cleavage, the 2′OH at the c^0 site is always used as the 2′OH* for both wild-type ribozyme and C-domain. For m^2 cleavage, the 2′OH at the c^0 site is always used as the 2′OH* for the wild-type ribozyme. This constraint is relaxed for the C-domain where the 2′OH at the m^2 site can be selected as 2′OH*.

To explain the positional shift of the 2′OH* in the C-domain reactions, we propose that the 2′OH* is selected by a combination of three regions of interactions. Two regions deal with ribozyme interactions with the tRNA component, and they select the 2′OH at the c^0 site to be utilized as 2′OH*. The dominant of the two involves the distal interactions, i.e., the T stem−loop in the tRNA. The distal interactions may function as a ruler to confine the 2′OH* selection within a very limited range. The other interaction involves the 3′CCA and the 1·72 base pair in the tRNA; they play a positive role in selecting the 2′OH (c^0) as the 2′OH* due to their relative positions in the pre-tRNA substrate.

In contrast, the third region involves ribozyme interactions with the 5′ leader which favor the selection of the 2′OH at the respective cleavage site to be utilized as 2′OH*. As discussed in our previous work, this third effect may be attributed to the optimal orientation of two motifs in the active site of the ribozyme (*11*). One motif binds the 2′OH* and is fixed for all cleavage sites. The other motif interacts with the 5′ three nucleotides to the respective cleavage site (i.e., nucleotides −3 to −1 for c^0 cleavage or −1 to +2 for m^2 cleavage, Figure 1B) and the scissile bond (c^0 or m^2 site). Since one of the two motifs is spatially fixed, both motifs have different juxtapositions for different cleavage sites in the ES complex. Presumably for a pre-tRNA substrate, the best orientation for the subsequent bond-breaking step is for the 2′OH* to coincide with the cleavage site.

This three-region model predicts that upon elimination of the dominant T stem−loop interaction through S-domain deletion, the 2′OH* selection would now depend on the relative magnitude of the 3′CCA/1·72 interaction to the 5′ leader interaction. If the distal interactions play no role in the selection of 2′OH*, cleavage by the C-domain and the wild-type ribozyme should have identical 2′OH* utilization. Our results clearly show that the location of 2′OH* changes upon S-domain deletion. Hence, the distal ribozyme−substrate interactions significantly contribute to the selection of 2′OH*.

DISCUSSION

Two ES Complexes in RNase P Catalysis. A comprehensive model including two ES complexes can be proposed to explain all the results described here:

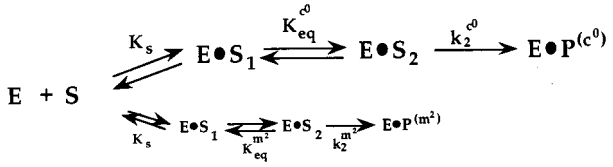

In this model, formation of ES_1 is determined by the concentration-dependent bimolecular collision of the substrate with the ribozyme (*25*, *38*). Only a subset of ribozyme−substrate interactions are present in ES_1, and these interactions determine the bimolecular binding constant (K_s) of the ribozyme−substrate complex. They include the interactions with the T stem−loop, the 5′ leader, and the 3′CCA/1·72 base pair in the pre-tRNA substrate. ES_1 undergoes a concentration-independent conformational change to allow additional ribozyme interactions with the 2′OH*, possibly the *pro-*R_p oxygen at the c^0 site (*11*, *39*), and maybe others. The ES_1-to-ES_2 transition corresponds to a conformational change and may not be pH dependent. k_2 corresponds to the Mg^{2+}-dependent bond-breaking step and is likely to be pH dependent. The observed cleavage rate at saturating ribozyme concentration (k_{cl}) is pH dependent. Therefore, it is likely that the equilibrium between ES_1 and ES_2 is established much faster than the k_2 step, so that $k_{cl} = [K_{eq}/(1 + K_{eq})]k_2$ (*21*). This model is supported by the following observations:

(*1*) *Location of the 2′OH* Relative to the Cleavage Site*. For the selected substrates and the miscleavage of the pre-tRNA substrate, the 2′OH* is not located at the cleavage site, but significantly affects the cleavage rate. Therefore, the location of the cleavage site does not determine the selection of the 2′OH*. Our model proposes that the 2′OH* interaction increases the equilibrium from ES_1 to ES_2. Since the 2′OH* can be located at one or more nucleotides away from the scissile bond, they are unlikely to participate directly in the bond-breaking step.

(*2*) *Differential Magnitude of 2′OH→2′H Effects.* Substitution of 2′OH* → 2′H produces the same qualitative, but significantly different quantitative effects for the P RNA and holoenzyme reactions. This result can be explained if the 2′OH* → 2′H substitution affects K_{eq}, but not the k_2 step. For the holoenzyme reaction, $K_{eq} \gg 1$, so that $K_{eq}/(1 + K_{eq})$ approximates 1. In such a case, even though the decrease in K_{eq} upon 2′OH → 2′H substitution is large, the observed decrease in the cleavage rate will not be proportional to the decrease in K_{eq}. For example, if K_{eq} of the wild-type substrate is approximately 35, a hypothetical decrease of K_{eq} by 1000-fold would only generate an observable effect of ∼30-fold. For the P RNA reaction, however, $K_{eq} < 1$, so that $K_{eq}/(1 + K_{eq})$ can approximate K_{eq}. In this case, a hypothetical decrease of K_{eq} by 1000-fold would generate an observable effect of ∼1000-fold.

(*3*) *Deletion of the S-Domain*. The S-domain deletion can be proposed to affect K_{eq}, but not the k_2 step. This hypothesis stems from the observed differential magnitude of the reactions with or without the P protein (∼40 versus ∼25 000-fold). In the presence of the P protein, the 2′OH* → 2′H substitution decreases the cleavage rate by ∼2200-fold for the C-domain reaction, in contrast to a decrease of only ∼30-fold for the same reaction by the holoenzyme. Presumably, the K_{eq} for the C-domain reaction with the P protein has dropped to much smaller than 1. Therefore, the cleavage rate for the C-domain with P protein is decreased by a much larger magnitude upon 2′OH* → 2′H substitution compared to the holoenzyme reaction. Without the P protein, the 2′OH* → 2′H substitution decreases the cleavage rate by the same ∼240-fold for reactions with the C-domain and the wild-type P RNA. Since the K_{eq} for the P RNA is less than 1 to begin with, a 2′OH* → 2′H substitution would have the same magnitude on the P RNA and the C-domain reactions. These results are consistent with the S-domain deletion and 2′OH* → 2′H substitution affecting the same event in the cleavage step.

A Structural Model for the ES_1-to-ES_2 Transition. Our structural model is based on the distal interactions playing a large role in determining the cleavage rate (Figure 3). In this model, the ES_1-to-ES_2 transition is strongly influenced by the orientation of the S- and C-domains of P RNA. There is little evidence for appreciable domain−domain interaction in the *B. subtilis* P RNA as demonstrated by hydroxyl radical protection and catalytic activity using both domains in trans [(*18*) and unpublished results]. Therefore, these domains may either be flexible to each other or have a different orientation in the absence of the P protein or a bound substrate. Binding of the P protein to both domains as indicated by hydroxyl radical protection (*11*) fixes the orientation of the domains for optimal binding of the biological substrates.

Formation of the ES_1 complex is a bimolecular process and depends on the concentration of the ribozyme and the substrate. Specific sites in the P RNA bind the T stem−loop, the 3′CCA, and the −1 to −3 nucleotides of a pre-tRNA substrate in the ES_1 complex. There are two major differences, however, between the ES_1 with or without the P protein. First, the P protein directly contacts the −4 to −7 nucleotides in the 5′ leader (*26*, *40*). This extra 5′ leader interaction increases the holoenzyme affinity for the substrate by >1000-fold under physiological conditions (*26*, *38*). Second, the P RNA binds to a larger area of the T stem−loop region than the area contacted by the holoenzyme. This extra T stem−loop interaction increases the P RNA affinity for the pre-tRNA substrate by ∼100-fold at high Mg^{2+} concentrations (*15*).

Formation of the ES_2 complex is concentration independent. Our model proposes little change in the domain orientation for the holoenzyme in the ES_1-to-ES_2 transition for c^0 cleavage, since the domains are already properly oriented upon P protein binding (Figure 3). Hence, the K_{eq} of the holoenzyme reaction is much larger than 1. In contrast, the P RNA−substrate complex undergoes a conformational change in two possible ways. The domain orientation in ES_2 can become identical to their counterpart in the holoenzyme. This reorientation loses the extra T stem−loop interaction and is therefore unfavorable. Alternatively, the T stem−loop interaction is maintained in ES_2. Instead, the structure of the linker region in the substrate can be changed to accommodate the altered domain−domain orientation. The second scenario

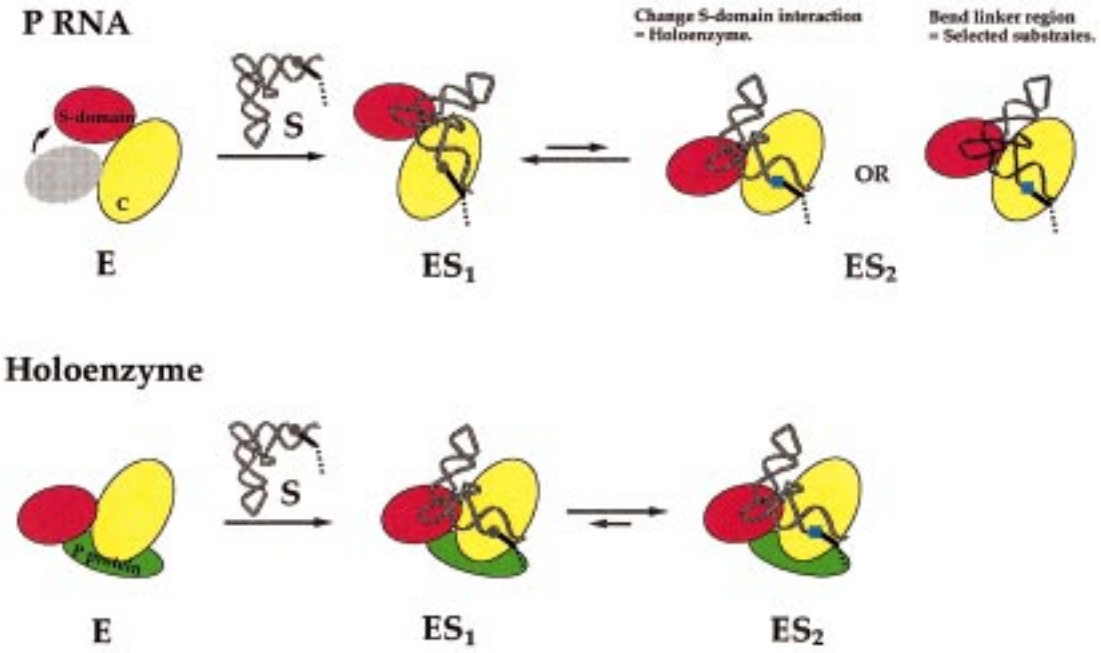

FIGURE 3: Structural model of the ES_1-to-ES_2 transition. Red, S-domain; yellow, C-domain; green, P protein; gray ribbon, the tRNA portion of the pre-$tRNA^{Phe}$ substrate; thick solid line, the −1 to −3 nucleotides in the 5′ leader; thick dashed line: the −4 to −7 nucleotides in the 5′ leader; shaded oval, location of the S-domain in the presence of P protein. The S-domain in the P RNA without the P protein may be dynamic. The 2′OH* is shown as a gray circle, and its interaction with the ribozyme is indicated by changing the gray circle to a blue square.

is consistent with the observation that in vitro selection performed with P RNA alone yielded substrates with much less structured linker regions compared to tRNA (*22*). Chemical modification showed that the coaxially stacked T stem and acceptor stem may become unstacked in a P RNA−tRNA complex (*41, 42*), suggesting that tRNA can change its structure in the linker region. This second way of reorientation disrupts the coaxially stacked T stem and the acceptor stem of tRNA and is again unfavorable. Therefore, the K_{eq} of the P RNA reaction is less than 1.

The purpose of the ES_1-to-ES_2 transition is to allow ribozyme interactions with 2′OH*, possibly the pro-R_p oxygen at the c^0 site in the pre-tRNA substrate, and maybe other functional groups to take place. The conformation of the ES_2 complex may be crucial in positioning the proposed Mg^{2+} ions in the active site to carry out the hydrolysis of the phosphodiester bond (k_2).

Involvement of the P Protein in the ES_2 Complex. As mentioned earlier, P protein binding may fix the orientation of the P RNA domains to favor the ES_2 complex. The P protein, however, also influences the choice of 2′OH* for c^0 and m^2 cleavage in a pre-tRNA substrate, possibly through its direct interaction with the 5′ leader. When the S-domain is deleted, the P protein may no longer be stably associated with the C domain (*12*). The only way for stable association of the P protein and the C-domain may be the binding of a pre-tRNA substrate to form a ternary complex. The P protein in the ternary complex can bind to −4 to −7 nucleotides in the ES complex destined for c^0 cleavage, but also to −5 to −1 nucleotides in the ES complex destined for m^2 cleavage. P protein binding to −5 to −1 may explain the significant utilization of the 2′OH (m^2) as the 2′OH* for m^2 cleavage (Table 4). P protein binding to −5 to −1 may also occur in the holoenzyme reaction when the c^0 site contains a 2′H and the 1•72 is not base paired (Table 3). Taken together, P protein in the holoenzyme is presumably restrained from direct interaction with the −5 to −1 nucleotides due to the steric restriction imposed by the T stem−loop binding to the S-domain *and* through ribozyme interaction with the 2′OH* at the c^0 site. These interactions can increase the fidelity of the holoenzyme reaction for biological substrates.

Comparison of the ES_1-to-ES_2 Transition to the Group I Ribozyme Reaction. Two distinct ES complexes, designated ES_{open} and ES_{closed}, are described in the group I ribozyme catalysis (reviewed by ref *4*). ES_{open} represents a concentration-dependent, bimolecular association of the ribozyme and the substrate to form the P1 helix. ES_{closed} represents a concentration-independent binding step of the P1 helix into the active site. The ES_1-to-ES_2 transition of the RNase P reaction is analogous to the ES_{open}-to-ES_{closed} transition in which additional ribozyme−substrate interactions take place. The interactions in ES_2 or ES_{closed} presumably allow precise positioning of the catalytic Mg^{2+} ions required for the bond-breaking step. The difference between RNase P and group I catalysis lies in the involvement of the substrate and the structural nature of this transition. The ES_{open}-to-ES_{closed} transition only requires the 5′ half of the substrate, whereas the ES_1-to-ES_2 transition requires the tRNA and the 5′ leader component of the substrate. The ES_{open}-to-ES_{closed} transition requires the movement of an RNA helix into a preformed binding cleft (*43*). The ES_1-to-ES_2 transition for the P RNA reaction may correspond to a change in orientation of the two independently folding domains and/or alteration of the linker region in the substrate. Absent in group I catalysis is the unique role of the P protein. Besides interacting directly with the 5′ leader, P protein may preorient the P RNA domains to be closer or even identical to their conformation in the ES_2 complex to significantly increase the cleavage step of this enzyme.

ACKNOWLEDGMENT

We thank Prof. Carol Fierke and Dr. S. Niranjanakumari for the P protein. We also thank Drs. Carl Correll, Tobin Sosnick, Xing-wang Fang, and one reviewer for helpful discussions and comments on the manuscript.

REFERENCES

1. Pley, H. W., Flaherty, K. M., and McKay, D. B. (1994) *Nature 372*, 68−74.
2. Scott, W. G., Finch, J. T., and Klug, A. (1995) *Cell 81*, 991−1002.
3. Wedekind, J. E., and McKay, D. B. (1998) *Annu. Rev. Biophys. Biomol. Struct. 27*, 475−502.
4. Narlikar, G. J., and Herschlag, D. (1998) *Annu. Rev. Biochem. 66*, 19−59.
5. Herschlag, D. (1992) *Biochemistry 31*, 1386−1399.
6. Wang, J.-F., Downs, W. D., and Cech, T. R. (1993) *Science 260*, 504−508.
7. Strobel, S. A., Ortoleva-Donnelly, L., Ryder, S. P., Cate, J. H., and Moncoeur, E. (1998) *Nat. Struct. Biol. 5*, 60−65.
8. Altman, S., Kirsebom, L., and Talbot, S. (1993) *FASEB J. 7*, 7−14.
9. Pace, N. R., and Brown, J. W. (1995) *J. Bacteriol. 177*, 1919−1928.
10. Guerrier-Takada, C., Gardiner, K., Marsh, T., Pace, N., and Altman, S. (1983) *Cell 35*, 849−857.
11. Loria, A., and Pan, T. (1998) *Biochemistry 37*, 10126−10133.
12. Loria, A., Niranjanakumari, S., Fierke, C. A., and Pan, T. (1998) *Biochemistry 37*, 15466−15473.
13. Smith, D., and Pace, N. R. (1993) *Biochemistry 32*, 5273−5281.
14. Steitz, T. A., and Steitz, J. A. (1993) *Proc. Natl. Acad. Sci. U.S.A. 90*, 6498−6502.
15. Loria, A., and Pan, T. (1997) *Biochemistry 36*, 6317−6235.
16. Pan, T. (1995) *Biochemistry 34*, 8458−8464.
17. Pan, T., and Jakacka, M. (1996) *EMBO J. 15*, 2249−2255.
18. Loria, A., and Pan, T. (1996) *RNA 2*, 551−563.
19. Fang, X.-W., Pan, T., and Sosnick, T. R. (1999) *J. Mol. Biol.* (submitted for publication).
20. Niranjanakumari, S., Kurz, J. C., and Fierke, C. A. (1998) *Nucleic Acids Res. 26*, 3090−3096.
21. Fersht, A. (1985) in *Enzyme structure and mechanism*, pp 98−120, W. H. Freeman and Co., New York.
22. Odell, L., Huang, V., Jakacka, M., and Pan, T. (1998) *Nucleic Acids Res. 26*, 3717−3723.
23. Kirsebom, L. A., and Svard, S. G. (1994) *EMBO J. 13*, 4870−4876.
24. LaGrandeur, T. E., Huttenhofer, A., Noller, H. F., and Pace, N. R. (1994) *EMBO J. 13*, 3945−3952.
25. Beebe, J. A., and Fierke, C. A. (1994) *Biochemistry 33*, 10294−10304.
26. Crary, S. M., Niranjanakumari, S., and Fierke, C. A. (1998) *Biochemistry 37*, 9409−9416.
27. Harris, M. E., Nolan, J. M., Malhotra, A., Brown, J. W., and Pace, N. R. (1994) *EMBO J. 13*, 3953−3963.
28. Pan, T., Loria, A., and Zhong, K. (1995) *Proc. Natl. Acad. Sci. U.S.A. 92*, 12510−12514.
29. Massire, C., Jaeger, L., and Westhof, E. (1998) *J. Mol. Biol. 279*, 773−793.
30. Sprinzl, M., Horn, C., Brown, M., Ioudovitch, A., and Steinberg, S. (1998) *Nucleic Acids Res. 26*, 148−153.
31. Quigley, G., and Rich, A. (1976) *Science 194*, 796−806.
32. Kim, S.-H. (1979) in *Crystal Structure of Yeast tRNA^{Phe} and General Structural Features of Other tRNAs* (Schimmel, P. R., et al., Eds.) pp 83−100 Cold Spring Harbor Laboratory Press, Cold Spring Harbor, NY.
33. Svard, S. F., and Kirsebom, L. A. (1992) *J. Mol. Biol. 227*, 1019−1031.
34. Holm, P. S., and Krupp, G. (1992) *Nucleic Acids Res. 20*, 421−423.
35. Kirsebom, L. A., and Svard, S. G. (1992) *Nucleic Acids Res. 20*, 425−432.
36. Pan, T., and Zhong, K. (1994) *Biochemistry 33*, 14207−14212.
37. Pan, T., Fang, X.-W., and Sosnick, T. R. (1999) *J. Mol. Biol. 286*, 721−731.
38. Kurz, J. C., Niranjanakumari, S., and Fierke, C. A. (1998) *Biochemistry 37*, 2393−2400.
39. Warnecke, J. M., Furste, J. R., Hardt, W.-D., Erdmann, V. A., and Hartmann, R. K. (1996) *Proc. Natl. Acad. Sci. U.S.A. 93*, 8924−8928.
40. Niranjanakumari, S., Stams, T., Crary, S. M., Christianson, D. W., and Fierke, C. A. (1998) *Proc. Natl. Acad. Sci. U.S.A. 95*, 15212−15217.
41. Kahle, D., Wehmeyer, U., and Krupp, G. (1990) *EMBO J. 9*, 1929−1937.
42. Gaur, R. K., Hanne, A., Conrad, F., Kahle, D., and Krupp, G. (1996) *RNA 2*, 674−681.
43. Golden, B. L., Gooding, A. R., Podell, E. R., and Cech, T. R. (1998) *Science 282*, 259−264.

BI990691F